Prolonged AICAR-induced AMP-kinase activation promotes energy dissipation in white adipocytes: novel mechanisms integrating HSL and ATGL

Mandeep P. Gaidhu, Sergiu Fediuc, Nicole M. Anthony, Mandy So, Mani Mirpourian, Robert L. S. Perry, and Rolando B. Ceddia[1]

School of Kinesiology and Health Science, York University, Toronto, Ontario, Canada

Abstract **This study was designed to investigate the effects of prolonged activation of AMP-activated protein kinase (AMPK) on lipid partitioning and the potential molecular mechanisms involved in these processes in white adipose tissue (WAT). Rat epididymal adipocytes were incubated with 5′-aminoimidasole-4-carboxamide-1-β-D-ribofuranoside (AICAR;0.5 mM) for 15 h. Also, epididymal adipocytes were isolated 15 h after AICAR was injected (i.p. 0.7 g/kg body weight) in rats. Adipocytes were utilized for various metabolic assays and for determination of gene expression and protein content. Time-dependent in vivo plasma NEFA concentrations were determined. AICAR treatment significantly increased AMPK activation, inhibited lipogenesis, and increased FA oxidation. This was accompanied by upregulation of peroxisome proliferator-activated receptor (PPAR)α, PPARδ, and PPARγ-coactivator-1α (PGC-1α) mRNA levels. Lipolysis was first suppressed, but then increased, both in vitro and in vivo, with prolonged AICAR treatment. Exposure to AICAR increased adipose triglyceride lipase (ATGL) content and FA release, despite inhibition of basal and epinephrine-stimulated hormone-sensitive lipase (HSL) activity. Here, we provide evidence that prolonged AICAR-induced AMPK activation can remodel adipocyte metabolism by upregulating pathways that favor energy dissipation versus lipid storage in WAT. Additionally, we show novel time-dependent effects of AICAR-induced AMPK activation on lipolysis, which involves antagonistic modulation of HSL and ATGL.**—Gaidhu, M. P., S. Fediuc, N. M. Anthony, M. So, M. Mirpourian, R. L. S. Perry, and R. B. Ceddia. **Prolonged AICAR-induced AMP-kinase activation promotes energy dissipation in white adipocytes: novel mechanisms integrating HSL and ATGL.** ***J. Lipid Res.*** **2009.** 50: **704–715.**

Supplementary key words obesity • AMP-activated protein kinase • adipose triglyceride lipase • hormone-sensitive lipase • PGC-1α • FA oxidation

Obesity is a major risk factor for metabolic disorders such as type 2 diabetes and cardiovascular disease, and it is characterized by the excessive accumulation of fat in the white adipose tissue (WAT). In this context, physiological and/or pharmacological strategies aimed toward increasing FA oxidation and energy dissipation in adipocytes have become of great therapeutic interest (1). One enzyme that has emerged as a potential target for dissipation of fat stores is AMP-activated protein kinase (AMPK). This enzyme functions as an energy sensor and is activated in response to changes to the AMP:ATP ratio in the cell (1, 2). Upon activation, AMPK switches on catabolic pathways to produce ATP in an attempt to restore cellular energy homeostasis. One pathway that is central to the integrated effects of AMPK in peripheral tissues is the stimulation of FA oxidation (1, 2), which could be of great relevance for the treatment of obesity and metabolic syndrome. However, currently very little is known regarding the effects of AMPK activation on glucose and lipid metabolism in WAT. We have recently reported that acute (1 h) 5′-aminoimidasole-4-carboxamide-1-β-D-ribofuranoside (AICAR)-induced AMPK activation in isolated rat adipocytes caused a reduction in glucose and FA uptake with concomitant reduction in oxidation of these substrates (3). This is contrary to the effects previously described in skeletal muscle (4), indicating that AMPK regulates glucose and lipid metabolism in a tissue-specific manner. Importantly, although acute AMPK activation can rapidly suppress glucose and FA uptake and metabolism in adipocytes (3), chronic AMPK activation has been associated with major alterations in gene expression, which might powerfully affect the ability of adipocytes to process glucose and FAs. In fact, it has been demonstrated that AMPKα2 is localized in the nuclei of many cells and is involved in the

This research was funded by the Natural Science and Engineering Research Council (NSERC), the Canadian Institute of Health Research (CIHR), and by the Canadian Diabetes Association through operating grants awarded to R.B.C. R.B.C. is also a recipient of the CIHR New Investigator Award. M.P.G. was supported by a CIHR Canadian graduate scholarship doctoral award. S.F. was supported by a doctoral NSERC post-graduate scholarship. Canadian graduate scholarships masters awards from CIHR and NSERC supported N.M.A. and M.S., respectively.

Manuscript received 8 September 2008 and in revised form 28 October 2008.

Published, JLR Papers in Press, December 2, 2008.
DOI 10.1194/jlr.M800480-JLR200

[1] To whom correspondence should be addressed.
e-mail: roceddia@yorku.ca

regulation of gene expression (5). Support for this comes from correlative in vivo studies reporting that chronic AMPK activation in hyperleptinemic rats is associated with increased expression of PGC-1α, higher mitochondrial content, upregulation of uncoupling proteins (UCPs), elevated expression of enzymes involved in β-oxidation, such as carnitine palmitoyl transferase 1 and acetyl-CoA oxidase, and decreased expression of lipogenic enzymes (acetyl-CoA carboxylase and fatty acid synthase) in WAT (6, 7). Observations from these studies suggest that because hyperleptinemia depletes body fat without increasing plasma FA levels, the upregulation of genes involved in oxidative metabolism are responsible for enhanced intra-adipocyte oxidation (6, 8). Even though these studies show that AMPK phosphorylation is increased by hyperleptinemia, a direct cause-effect relationship between AMPK activation and these metabolic changes in adipocytes has not been established (6, 8). Importantly, the effects of hyperleptinemia require the presence of a functional leptin receptor that engages many downstream targets, not specifically AMPK. In order to extend the knowledge on the role of AMPK activation in adipocyte metabolism, we tested whether chronic activation of AMPK causes alterations in gene expression that promote energy dissipation rather than storage in adipocytes. This is particularly important because potential pharmacological strategies for the treatment of obesity and its related metabolic disorders by selectively targeting adipose tissue AMPK activation will be chronic rather than acute in nature. Therefore, in order to test whether chronic activation of AMPK can lead to metabolic alterations that promote energy dissipation in WAT, we performed in vivo and in vitro studies to assess various parameters as well as the potential mechanisms involved in the regulation of glucose and lipid metabolism by AMPK in adipocytes. Here, we provide novel evidence that chronic AICAR-induced AMPK activation causes a potent anti-lipogenic effect by increasing the expression of PGC-1α, peroxisome proliferator-activated receptor (PPAR)α, and PPARδ, by suppressing FA uptake and by promoting oxidation of this substrate in rat white adipocytes. Chronic AICAR-induced AMPK activation also increased adipose triglyceride lipase (ATGL) content and FA release, despite the fact that basal and epinephrine-stimulated hormone-sensitive lipase (HSL) phosphorylation and activity were suppressed in adipocytes. Our data indicate that through chronic AMPK activation, WAT metabolism can be remodeled toward energy dissipation, and this may be of great relevance for the treatment of obesity and its related metabolic disorders.

MATERIALS AND METHODS

Reagents

AICAR was purchased from Toronto Research Chemicals, Inc. (Toronto, Ontario, Canada); cardiolipin, *Escherichia coli* diacylglycerol (DAG) kinase, DETAPAC, DTNB, di-'isononyl' phthalate, epinephrine, FA-free BSA, free glycerol determination kit, glucose oxidase kit, MTT toxicology assay kit, octyl-β-glucoside, oxaloacetic acid, palmitic acid, phenylethylamine, silica-coated TLC plates, and SYBR green were obtained from Sigma; [1-^{14}C]diolein, [9,10-^{3}H]triolein, [U-^{14}C]glycerol and [γ-^{32}P]ATP were purchased from American Radiolabeled Chemicals, Inc. (St. Louis, MO); D-[U-^{14}C]glucose, [1-^{14}C]pyruvic acid, and [1-^{14}C]palmitic acid were from GE Healthcare Radiochemicals (Quebec City, Quebec, Canada); and human insulin (Humulin) was from Eli Lilly. NEFA kit was from Wako Chemicals. Lactate oxidase kit was from Trinity Biotech. RNeasy lipid extraction kit was from Qiagen. Superscript II and Taq polymerase were from Invitrogen. DNase kit was from Ambion. Tripalmitin, triolein, and *sn*-1,2-dioleoylglycerol standards were purchased from Nu Check Prep (Elysian, MN). Phosphatidic acid standard was from Avanti Polar Lipids (Alabaster, AL). Specific antibodies against phospho-AMPK, AMPK, acetyl-CoA carboxylase (ACC), HSL, phospho-HSL (all residues), and ATGL were from Cell Signaling Technology, Inc. (Beverly, MA). Phospho-ACC antibody was from Upstate (Charlottesville, VA). Phosphoenolpyruvate carboxykinase-1(PEPCK-1) and GAPDH were from Abcam (Cambridge, MA). All other chemicals were of the highest grade available.

Animals and isolation of primary adipocytes

Male albino rats (Wistar strain), weighing 150–200 g, were maintained on a 12/12 h light/dark cycle at 22°C and fed (ad libitum) standard laboratory chow. The experimental protocol was approved by the York University Animal Care Ethics Committee. Rat epididymal fat pads were quickly removed, finely minced, and digested at 37°C for 30 min in DMEM containing type II collagenase (1 mg/ml). The digested tissue was filtered through a nylon mesh, and washed three times with DMEM supplemented with 1% FBS, 1% antibiotic/antimycotic, 50 μg/ml gentamycin, and 15 mM HEPES (DMEM-1% FBS) (3). Cells were resuspended in DMEM-1% FBS, and incubated in the absence or presence of AICAR (0.5 mM) for 15 h prior to assaying for various metabolic parameters. The amount of AICAR chosen for our in vitro studies was based on a dose response with concentrations of 0, 0.25, 0.5, 1, and 2 mM, where AMPK activation was detectable using 0.5 mM.

MTT assay for cytotoxicity

The 3-[4,5-dimethylthiazol-2-yl]2,5-diphenyl tetrazolium bromide (MTT) cytotoxicity test was performed according to the manufacturer's instructions with slight modifications, as described by Canová et al. (9). Briefly, cells were incubated for 15 h in the absence or presence of AICAR (2 mM). Subsequently, cells were resuspended in serum and phenol red-free DMEM and cultivated for 2 h in MTT work solution, consisting of a final concentration of 500 μg/ml MTT. The resulting purple formazan crystals were solubilized using the solution provided, and measured spectrophotometrically at 540 nm.

Measurement of glycerol kinase activity

Adipocytes were incubated for 15 h in the presence of either AICAR (0.5 mM) or rosiglitazone (1 μM). Control cells received

TABLE 1. Citrate synthase activity

Condition	Citrate Synthase Activity
	nmol/min/μg protein
Control	2.42 ± 0.53
AICAR	4.68 ± 0.36[a]

AICAR, 5′-aminoimidasole-4-carboxamide-1-β-D-ribofuranoside. Cells were incubated in the absence or presence of AICAR (0.5 mM) for 15 h, and protein was extracted for determination of citrate synthase activity. Values were corrected for microgram of protein per sample and were expressed as mean ± SEM. Data were compiled from two independent experiments, with a sample size of n = 8. Unpaired *t*-test was performed for statistical analysis.

[a] $P < 0.05$ versus control.

only vehicle (DMEM-1% FBS or DMSO). After incubation, cells were snap-frozen in liquid nitrogen and prepared for measurement of glycerol kinase (GyK) activity (10). Briefly, 150 μl of extraction buffer (50 mM HEPES, 40 mM KCl, 11 mM $MgCl_2$, 1 mM EDTA, 1 mM dithiothreitol, pH 7.8) was added to cells, which were then vortexed and sonicated for complete lysis. Homogenates were centrifuged, and the infranatant containing GyK was collected. Samples of the extract containing 10 μg of total protein were added to 75 μl assay buffer containing 5 μCi/ml of U-[^{14}C] glycerol (~30 μM), for 3 h at 37°C. The reaction was terminated by the addition of 150 μl of 97% ethanol, 3% methanol (10). Seventy-five microliters of the alcohol-treated reaction mixture was spotted onto DE-81 Whatman filters and allowed to air dry before being washed with distilled water overnight. Filters were dried again and counted for radioactivity (10).

Measurement of glycerol, glucose, and pyruvate incorporation into lipids

For glycerol, glucose, and pyruvate incorporation into lipids, adipocytes (~2 × 10^5) were preincubated with AICAR for 15 h and subsequently exposed for 1 h to either [U-^{14}C]glycerol (0.5 μCi/ml; ~30 μM), D-[U-^{14}C]glucose (0.5 μCi/ml, with 5.5 mM unlabeled D-glucose), or [1-^{14}C]pyruvic acid (0.1 μCi/ml, with 10 μM unlabeled pyruvate) to allow incorporation of these substrates into total lipids (3, 4). Subsequently, lipids were extracted

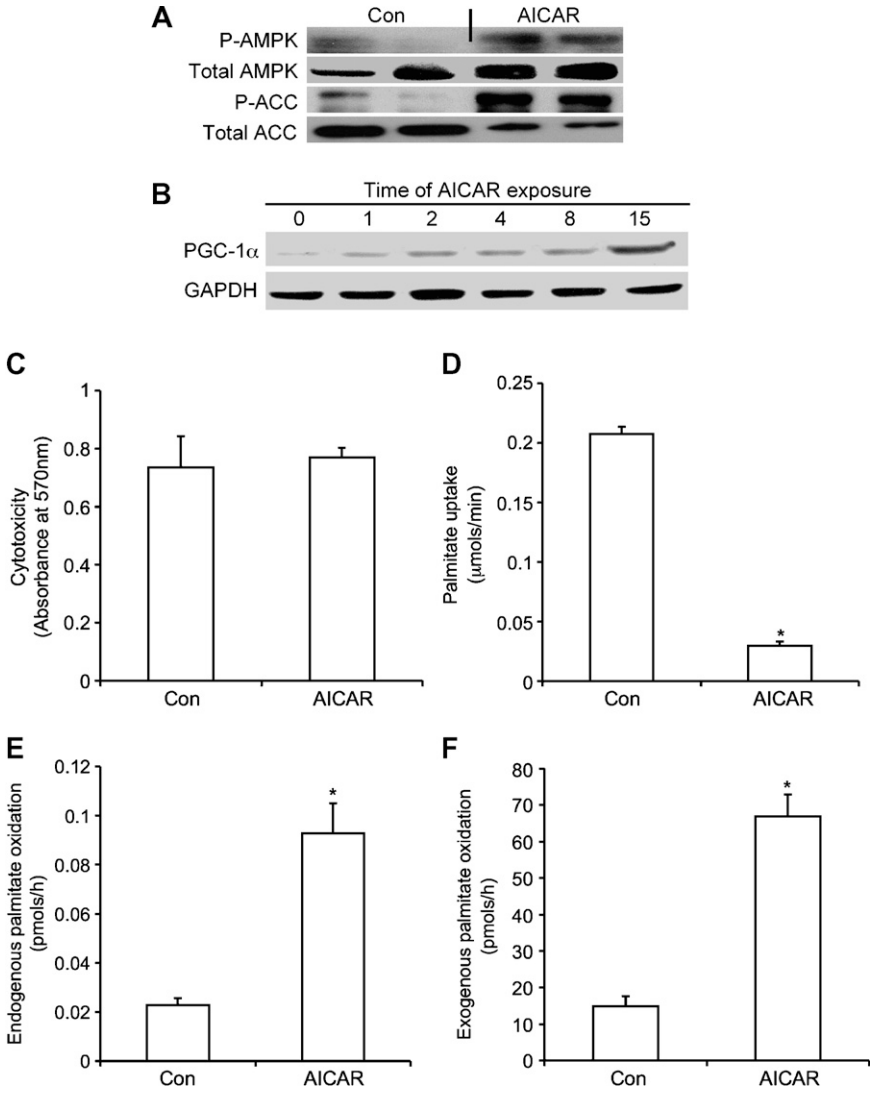

Fig. 1. Effects of 5′-aminoimidasole-4-carboxamide-1-β-D-ribofuranoside (AICAR) on content and phosphoryation of AMP-activated protein kinase (AMPK) and acetyl-CoA carboxylase (ACC) (A), PGC-1α content (B), cytotoxicity (C), palmitate uptake (D), and $^{14}CO_2$ production from [1-^{14}C]palmitic acid via endogenous (E) and exogenous (F) sources. Cells were treated in vitro for 15 h with AICAR (0.5 mM) prior to assays. For endogenous oxidation, 1 μCi/ml of [1-^{14}C]palmitic acid was incorporated into adipocytes 30 min prior to assaying for oxidation, and washed four to six times to eliminate unincorporated [1-^{14}C]palmitic acid. For exogenous oxidation, 0.2 μCi/ml of [^{14}C]palmitic acid was present in the media. Data shown do not contain L-carnitine in the media. Blots are representative of three independent experiments. Data for cytotoxicity, uptake, and oxidation were compiled from four to five independent experiments, with n = 12–16 for each condition. Unpaired *t*-tests were performed for statistical analyses. Error bars represent SEM. *$P < 0.05$ versus control (Con) conditions.

using the method of Dole and Meinertz (11) and assessed for radioactivity (3, 4).

Incorporation of [1-^{14}C]palmitic acid into triacylglycerols

After the 15 h incubation in the absence or presence of AICAR, adipocytes ($\sim 2 \times 10^5$) were incubated with 0.2 mM palmitic acid and 0.2 μCi/ml of labeled [1-^{14}C]palmitic acid for 1 h to allow incorporation of palmitate into lipids (12). Subsequently, lipids were extracted by the method of Bligh and Dyer (13) with a few modifications. Briefly, cells were lysed in 0.5 ml of methanol with vigorous vortexing, and lipids were extracted by adding 1.5 ml of a chloroform-methanol solution (1:2, v/v) and incubated on ice for 1 h. Subsequently, 0.5 ml each of chloroform and 0.2 M NaCl were added to the tubes, and phases were separated by centrifugation. The bottom phase was removed and washed with 0.5 ml each of methanol and NaCl. The lower phase was extracted and evaporated under a constant stream of N_2. Lipids were then resuspended in 40 μl of a chloroform-methanol solution (2:1), and 5 μl was spotted onto a silica-coated glass TLC plate with triacylglycerol standards (tripalmitin and triolein). Lipids were separated with *n*-hexane-ethyl ether-acetic acid (70:30:1) as solvent and visualized using iodine vapor. The spots corresponding to the triacylglycerol (TAG) standards were scraped off and counted for radioactivity.

Palmitate uptake

Palmitate uptake was assayed as described previously (3) with a few modifications. Briefly, fat cells (2×10^5) were resuspended to a lipocrit of 30% and incubated either in the absence or presence of AICAR for 15 h. Subsequently, palmitic acid uptake was assayed in Krebs Ringer buffer (KRB) containing [1-^{14}C]palmitic acid (0.2 μCi/ml) and nonlabeled palmitate (30 μM) conjugated with FA-free albumin in a molar ratio of 1 (~0.7% albumin). After cells had been exposed to the assay buffer for 3 min, an aliquot (240 μl) of the cell suspension was transferred to microtubes containing 100 μl of cold di-'isononyl' phthalate and quickly centrifuged (13,000 rpm for 30 s) to separate the cells from the radiolabeled incubation medium and to terminate the reaction. Microtubes were cut through the oil phase, and cells were transferred to scintillation vials to be counted for radioactivity. Nonspecific transport was determined in the same conditions, except that ice-cold assay buffer was added to the cells and immediately centrifuged (time zero). Nonspecific values were subtracted from all conditions.

Determination of lipolysis and the production of $^{14}CO_2$ from exogenous and endogenous [1-^{14}C]palmitic acid

Lipolysis was determined after AICAR-treated adipocytes ($\sim 2 \times 10^5$) had been incubated for 75 min in the absence or presence of epinephrine (100 nM final concentration) or vehicle (0.5 M HCl). An aliquot of the media (400 μl) was collected and analyzed for glycerol and NEFA release using commercially available kits from Sigma Aldrich and Wako Chemicals, respectively. The oxidation of exogenous palmitate by isolated adipocytes preincubated with AICAR for 15 h was measured in KRB containing 4% FA-free albumin in the presence of 0.2 mM palmitic acid and 0.2 μCi/ml of labeled [1-^{14}C]palmitic acid for 1 h (3). For endogenous palmitate oxidation, cells were incubated in the absence or presence of AICAR for 15 h. Subsequently, cells were prelabeled with 1 μCi/ml of [1-^{14}C]palmitic acid (12, 14) for 30 min, and then washed to eliminate any [1-^{14}C]palmitic acid that had not been incorporated into adipocytes. Cells were then incubated in KRB containing 4% FA-free albumin, and $^{14}CO_2$ was collected as previously described for measurement of oxidation (3).

Citrate synthase activity

Citrate synthase activity was assayed with adaptations to the method described elsewhere (15). Adipocytes (6×10^6) were lysed in buffer (25 mM Tris-HCl, 1 mM EDTA, pH 7.4) and centrifuged, and the infranatant was collected. An aliquot containing ~20 μg of protein was added to the assay buffer (50 mM Tris-HCl, pH 8.1, 0.2 mM DTNB, 0.1 mM acetyl-CoA, 0.5 mM oxaloacetate), and absorbance was measured over 10 min in a spectrophotometer at 412 nm. The assay control contained all components except the sample, and its value was subtracted from all conditions.

Quantification of DAG content

DAG levels were quantified by a modified enzymatic method described by Preiss et al. (16), which is based on the principle of DAG phosphorylation and conversion into phosphatidic acid. Briefly, control and AICAR-treated adipocytes (1×10^5) were lysed, and lipids were extracted as described above. Lipids were dried under N_2 gas, and solubilized in 80 μl of a 7.5% octyl-β-D-glucoside, 5 mM cardiolipin in 1 mM DETAPAC solution using brief sonication. Subsequently, 60 μl of reaction buffer (100 mM imidazole HCl, pH 6.6, 100 mM NaCl, 25 mM $MgCl_2$, and 2 mM EGTA), 10 μl of 20 mM DTT in 1 mM DETAPAC, and 10 μl of DAG kinase solution (~4 μg per reaction) were added to 10 μl of solubilized lipids. Reactions were initiated with the addition of 10 μl of ATP solution (final concentrations 1 mM ATP and 2 μCi

TABLE 2. Quantitative PCR analysis of mRNA expression

Gene	Primer Sequences (5′ → 3′)	Fold Increase Relative to Control
AMPKα1	F - ACCATTCTTGGTTGCCGAAACACC R - CCAAATGCCACTTTGCCTTCCGTA	1.03 ± 0.08
AMPKα2	F - CAGCCCTTGGGCATCTTTGCTAAT R - AAAGACCCTATGGCCAAAGCAAGG	4.79 ± 0.31[a]
PGC-1α	F - ACCGTAAATCTGCGGGATGATGGA R - CATTCTCAAGAGCAGCGAAAGCGT	3.04 ± 0.18[a]
PEPCK-1	F - TCCGAAGTTGGCATCTGACACTGA R - CTCACACACACATGCTCACACACA	7.02 ± 0.61[a]
PEPCK-2	F - AGGCTGGAAAGTGGAGTGTG R - GTGGAAGAGGCTGGTCAATG	0.71 ± 0.06
UCP-1	F - TCAACACTGTGGAAAGGGACGACT R - TCTGCCAGTATGTGGTGGTTCACA	1.29 ± 0.26
UCP-2	F - AGCACATCTCACTATGCCTCCTCA R - ACATTGGAGCTTGCTTTATGGGCG	0.73 ± 0.10
PPARα	F - TGCAGGTCATCAAGAAGACCGAGT R - TGTGCAAATCCCTGCTCTCCTGTA	3.70 ± 0.56[a]
PPARδ	F - AGACCTCAGGCAGATTGTCACAGA R - ACACTTTGTCAGCGACTGGGACTT	2.50 ± 0.33[a]
PPARγ	F - ACACTTTGTCAGCGACTGGGACTT R - AGACCTCAGGCAGATTGTCACAGA	2.97 ± 0.37[a]
COX-8	F - ATGGTTCCAGCAGGATGGGTCTTA R - AGCGTTTAATTGGCCTCTCAGGGA	2.18 ± 0.19[a]
COX-6	F - TTGCTGCTGCCTATAAGTTTGGCG R - AGTTCAGGAACACAGGTCAGCAGT	1.68 ± 0.13[a]
CPT-1a	F - ACGGACCCTCGTGATACAAACCAA R - AGCCAAGGCATCTCTGGATGTAGT	0.81 ± 0.18
CPT-1b	F - AGCCCTTAGGTGCCTATGTTTGGT R - ACAGCACTCTCGAAGTCCGCATTA	3.94 ± 0.56[a]
Acetyl-CoA oxidase	F - AGATTAGCCAGGAAAGCCGACCAT R - TCCTTCGTGGATGAAGTCCTGCAA	2.27 ± 0.15[a]

F, forward; R, reverse. Total RNA was extracted from adipocytes after 15 h of AICAR treatment and subsequently used for quantitative PCR analysis. GAPDH was used as the control gene. N = 4–5 for each group. Samples were run in triplicates on the plate. Data are given as mean ± SEM.

[a] $P < 0.05$ versus control.

of [γ-^{32}P]ATP per reaction) and allowed to proceed at 25°C for 30 min. The reaction was terminated with the addition of 2 ml of cold chloroform-methanol (1:2) solution, followed by 1 ml of 0.2 M NaCl and 2 ml of chloroform. Tubes were vortexed, and after separation of phases, the lower phase was carefully extracted and placed into fresh test tubes. Lipids were dried under N_2 gas and solubilized in 50 μl of 5% methanol in chloroform. Five microliters of the lipid was spotted onto a silica-coated glass plate and separated using a solvent composed of chloroform, acetone, methanol, acetic acid, and distilled water (50:20:10:10:5, v/v/v/v/v). As a standard, cold phosphatidic acid (25 μg) was spotted onto the plate. Lipids were visualized using iodine vapor, corresponding spots were scraped off, and radioactivity was counted. For absolute quantification of DAG, a standard curve with known amounts of *sn*-1,2-dioleoylglycerol was assayed concurrently with samples for each experiment. Nonspecifics were treated the same as standards and samples, except that no lipid was present. Nonspecific values were subtracted from all values.

Western blot analysis

AICAR-treated and control adipocytes (1×10^7) were stimulated with epinephrine (100 nM) for the final 30 min of the 15 h incubation period. For time course analyses, cells were exposed to AICAR for 0, 1, 2, 4, 8, and 15 h. Cells were then immediately snap-frozen in liquid nitrogen and lysed in buffer composed of 25 mM Tris-HCl and 25 mM NaCl, (pH 7.4), 1 mM $MgCl_2$, 2.7 mM KCl, 1% NP-40, and protease and phosphatase inhibitors (0.5 mM Na_3VO_4, 1 mM NaF, 1 μM leupeptin, 1 μM pepstatin, 1 μM okadaic acid, and 20 mM PMSF) (3, 17). Cell lysates were centrifuged, the infranatant was collected, and an aliquot was used to determine protein concentration using the Bradford method. Sample preparation and SDS-PAGE conditions were performed as previously described (3). All primary antibodies were used in a dilution of 1:1,000 with the exception of AMPK (1:500), PGC-1α (1:200), and GAPDH (1:5,000).

Quantitative PCR analysis

Total RNA was isolated from adipocytes using the RNeasy kit, followed by DNase treatment in order to remove genomic DNA carry-over. Primers were designed using the software PrimerQuest (IDT) based on probe sequences available at the Affymetrix database (NetAffx™ Analysis Center, http://www.affymetrix.com/analysis) for each given gene. Real-time PCR reactions were carried out at amplification conditions as follows: 95°C (3 min); 40 cycles of 95°C (10 s), 65°C (15 s), 72°C (20 s); 95°C (15 s), 60°C (15 s), 95°C (15 s). Quantitative PCR was performed using the ABI Prism® 7900HT Sequence Detection System (Applied Biosystems, Perkin Elmer). All genes were normalized to the control gene GAPDH and β-actin, and values are expressed as fold increases relative to control. Primers sequences are shown in **Table 1**.

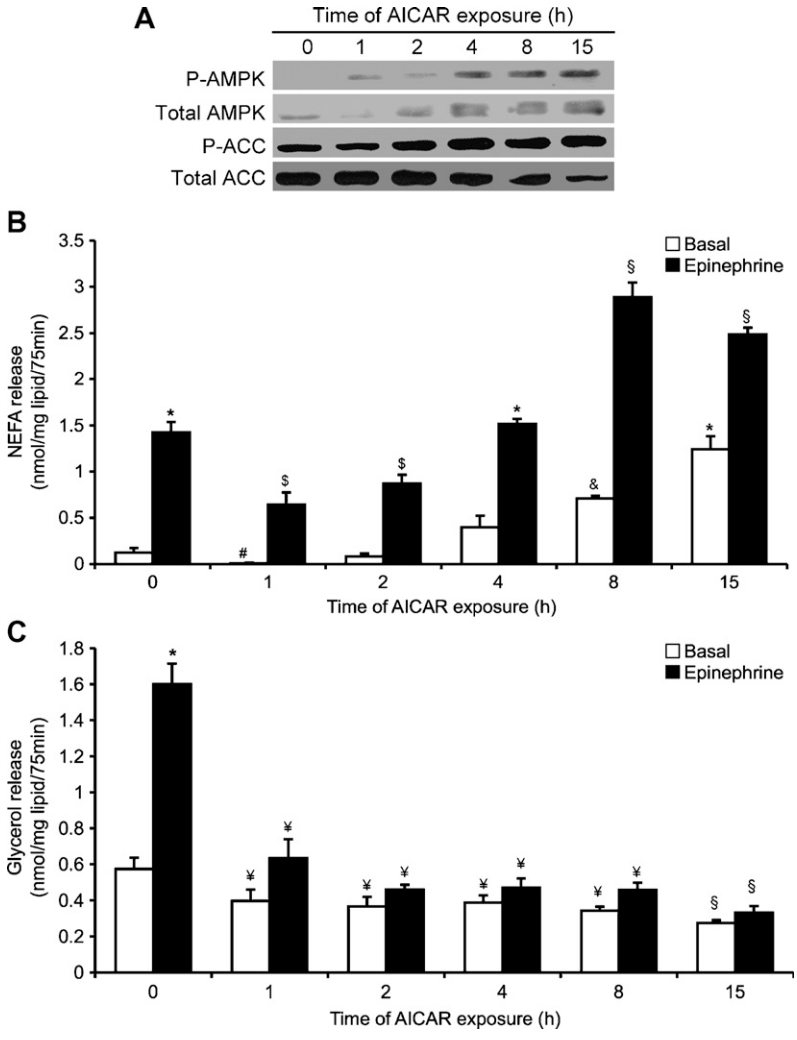

Fig. 2. Time-dependent effects of AICAR on content and phosphorylation of AMPK and ACC from 0 to 15 h (A). Time-dependent effects of AICAR and epinephrine on NEFAs (B) and glycerol release (C) in vitro. Basal and epinephrine conditions are denoted as white and black bars, respectively. Adipocytes were preincubated with AICAR (0.5 mM) for various time periods (0 to 15 h) prior to epinephrine stimulation (100 nM) for 75 min. Blots are representative of three independent experiments. Data for NEFA and glycerol determination were compiled from three independent experiments, with n = 12–15 for each condition. Two-way ANOVAs were performed for statistical analyses. Error bars represent SEM. $^{*}P < 0.05$ versus all other conditions; $^{\#}P < 0.05$ versus all other conditions; $^{\$}P < 0.05$ versus 0, 4, 8, and 15 h; and $^{\&}P < 0.05$ versus basal 0, 1, 2, 4, and 15 h and epinephrine 8 h and 15 h; $^{\S}P < 0.05$ versus all other conditions; $^{¥}P < 0.05$ versus 0 h and 15 h.

In vivo treatment

Rats were given a single intraperitoneal injection of either saline or AICAR (0.7 g/kg body weight). The dosage was chosen based on previous in vivo rat studies that used between 0.5 and 1.0 g/kg body weight for chronic AICAR injections (18–20). Fifteen hours later, epididymal fat pads from each group were extracted, and adipocytes were isolated for analysis of palmitate oxidation (3) or protein expression by Western blotting. For in vivo glucose and NEFA determination, animals were injected with either saline or AICAR, and blood samples from the saphenous vein were collected at various time points. An 8 h time course was chosen for in vivo studies to avoid the effects of circadian rhythm on lipolytic rate (21). Glucose concentration was determined by the glucose oxidase method using a commercially available kit from Sigma.

HSL and TAG lipase activity

Activity of HSL was measured as established by Fredrikson et al. (22). Briefly, after treatment with AICAR for 15 h, cells were stimulated with epinephrine (100 nM) for 75 min. Subsequently, cells were lysed in 2 vols of homogenization buffer (22) and centrifuged for 45 min (4°C, 11,000 *g*). An aliquot (~100 μg protein) of the infranatant was incubated with assay buffer containing a final concentration of 7.5 mM unlabeled diolein and 0.5 μCi/ml of labeled [1-^{14}C]diolein at 37°C for 10 min. This substrate is a commercially available diacylglycerol that liberates a labeled [1-^{14}C]oleic acid in the presence of HSL activity (22). The reaction was terminated with the addition of 3.25 ml of extraction buffer and 1.05 ml of a 0.1 M K_2CO_3, 0.1M boric acid solution (22). Tubes were centrifuged (800 *g*), and 1 ml from the upper phase, which contained the liberated [1-^{14}C]oleic acid, was extracted and counted for radioactivity. Determination of TAG lipase activity was identical to measurement of HSL activity, except that the assay buffer contained 5 mM unlabeled triolein and 0.5 μCi/ml of labeled [9,10-^{3}H]triolein as a substrate.

Statistical analysis

Statistical analyses were performed by unpaired *t*-tests or using either one- or two-way ANOVA with Tukey-Kramer multiple comparison posthoc tests as noted in each figure. The level of significance was set to $P < 0.05$.

RESULTS

AMPK and ACC phosphorylation and content, PGC-1α content, cytotoxicity, palmitate uptake, palmitate oxidation, and citrate synthase activity

Adipocytes treated with AICAR for 15 h elicited an increase in both phosphorylation and content of AMPK (**Fig. 1A**). AICAR increased ACC phosphorylation, whereas total ACC levels decreased relative to control values

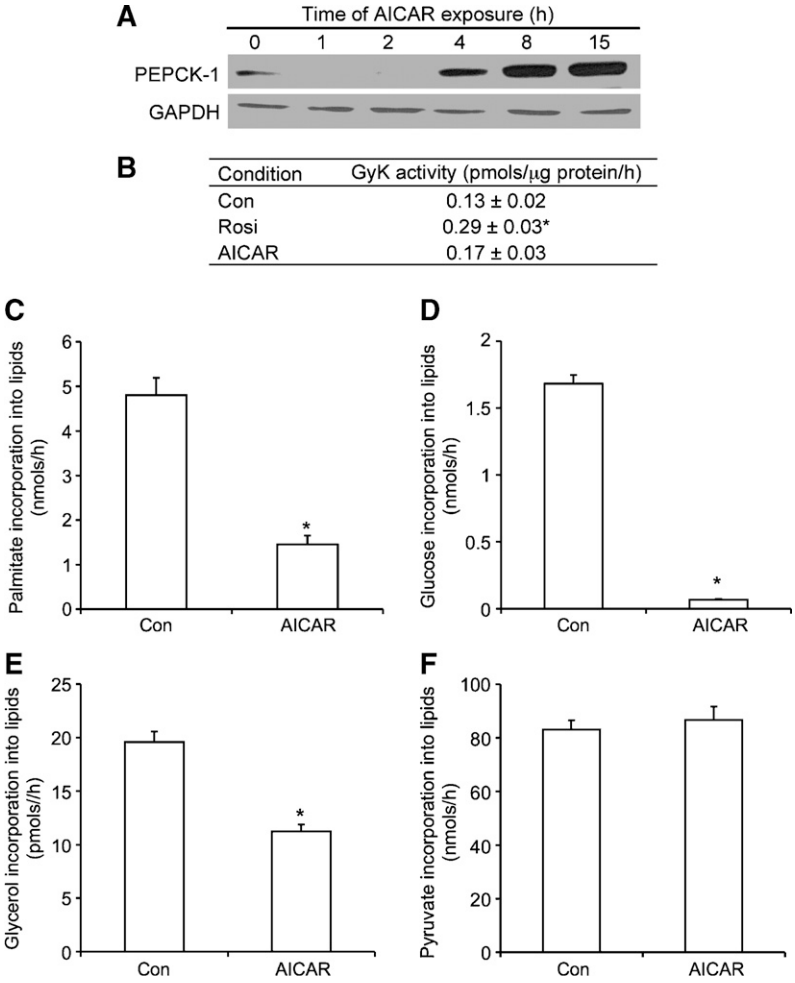

Fig. 3. Measurement of PEPCK content by Western blotting (A), glycerol kinase (GyK) activity (B), and the incorporation of palmitate (C), glucose (D), glycerol (E), and pyruvate (F) into lipids. Cells were incubated in the absence (Con) or presence of AICAR (0.5 mM) for 15 h and assayed for incorporation of various substrates ([1-^{14}C]palmitic acid, D-[^{14}C]glucose, [U-^{14}C]glycerol, and [1-^{14}C]pyruvic acid) into lipids. Rosiglitazone (Rosi; 1 μM) was used as a positive control. PEPCK blot is representative of two independent experiments. All other data were compiled from three to four independent experiments, with n = 12–15 for each condition. Unpaired *t*-tests and one-way ANOVAs were performed for statistical analyses. Error bars represent SEM. *$P < 0.05$ versus Con.

(Fig. 1A). PGC-1α content clearly increased after 15 h of AICAR treatment (Fig. 1B). Measurement of cytotoxicity revealed no difference between control and adipocytes exposed to AICAR for 15 h (Fig. 1C). Palmitate uptake significantly decreased (~60%) in AICAR-treated cells (Fig. 1D), whereas oxidation of both endogenous and exogenous palmitate was elevated by ~6.6- and ~3-fold, respectively (Fig. 1E, F). We also tested whether the addition of L-carnitine to the incubation medium would modify the ability of fat cells to oxidize long-chain FAs. We exposed isolated adipocytes to AICAR for 15 h in the absence or presence of carnitine (500 μM). The addition of L-carnitine increased palmitate oxidation from 0.021 ± 0.004 to 0.058 ± 0.004 nmol/h and from 0.052 ± 0.007 to 0.150 ± 0.004 nmol/h in control and AICAR-treated cells, respectively. These data indicate that although the addition of L-carnitine to the incubation medium increased the absolute values of palmitate oxidation, it did not alter the AICAR-induced ~3.0-fold increase in the ability of adipocytes to oxidize palmitate. Compatible with the elevation in oxidation, AICAR-treated cells also elicited an increase in citrate synthase activity by ~1.9-fold relative to control cells (Table 1).

Quantitative PCR analysis

Quantitative PCR analysis revealed that the mRNA levels of the α1 isoform of AMPK were not altered by AICAR treatment, whereas the expression of the α2 isoform increased by ~4.8-fold (**Table 2**). Additionally, mRNA levels of PGC-1α, PEPCK-1, PPARα, PPARδ, and PPARγ were increased by ~3.0-, ~7.0-, ~3.7-, ~2.5-, and ~2.8-fold, respectively, after AICAR treatment (Table 2). Enzymes involved in β-oxidation, such as carnitine palmitoyltransferase-1b (CPT-1b) and acetyl-CoA oxidase, were upregulated by ~3.9- and 2.3-fold, respectively. Expression of PEPCK-2, UCP-1, and UCP-2 remained unaltered with AICAR treatment (Table 2).

In vitro lipolysis

NEFAs in the medium decreased after 1 h and 2 h of AICAR treatment under both basal (~95% and ~35%, respectively) and epinephrine-stimulated (~55% and ~40%, respectively) conditions (**Fig. 2B**). After 4, 8, and 15 h of AICAR treatment, basal NEFA levels increased by ~3.2-, ~5.8-, and ~10-fold, whereas under epinephrine-stimulated conditions, this variable increased by ~1.1-, ~2-, and ~1.8-fold, respectively (Fig. 2B). Glycerol release was suppressed

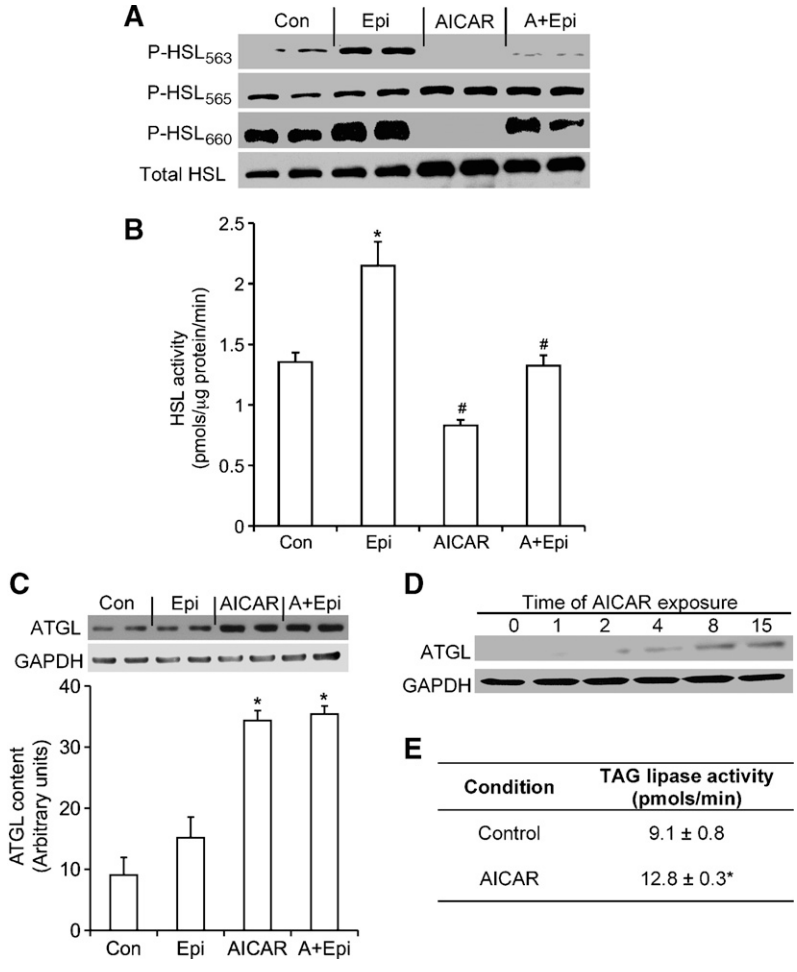

Fig. 4. Effects of AICAR, epinephrine (Epi), and AICAR plus epinephrine (A+Epi) on content and phosphorylation of hormone-sensitive lipase (HSL) at serine residues 563, 565, and 660 (A). Measurement of HSL activity (B), adipose triglyceride lipase (ATGL) content (C) and (D), and triacylglycerol (TAG) lipase activity (E). For Western blots, adipocytes were either incubated with AICAR (0.5 mM) for various time points, or preincubated with AICAR for 15 h and subsequently exposed to epinephrine (100 nM) for 30 min. Cells were lysed and prepared for Western blotting analysis as described in Materials and Methods. HSL activity was measured by preincubating cells with AICAR for 15 h and stimulating them with epinephrine for 75 min prior to assay. Blots are representative of three to four independent experiments. Data for HSL activity were compiled from three independent experiments, with n = 10–12 for each condition. One-way ANOVAs were performed for statistical analyses. Error bars represent SEM. $^{*}P < 0.05$ versus all other conditions; $^{\#}P < 0.05$ versus Con and Epi.

at all time points, remaining at ~50% and 20% of control values for basal and epinephrine conditions, respectively (Fig. 2C).

PEPCK-1 content, GyK activity, and incorporation of palmitate, glucose, glycerol, and pyruvate into lipids

PEPCK-1 content was increased in a time-dependent manner with AICAR treatment (**Fig. 3A**). Rosiglitazone was used as a positive control (10), and as expected, it significantly increased GyK activity by ~60% (Fig. 3B). AICAR treatment did not change the activity of this enzyme (Fig. 3B). AICAR treatment inhibited incorporation of palmitate, glucose, and glycerol into lipids by ~70, ~90, and ~35%, respectively (Fig. 3C–E), whereas the incorporation of pyruvate into lipids remained unaffected (Fig. 3F).

HSL content, phosphorylation, and activity, ATGL content, and TAG lipase activity

As expected, phosphorylation of HSL_{563} and HSL_{660} increased with epinephrine stimulation (**Fig. 4A**). AICAR

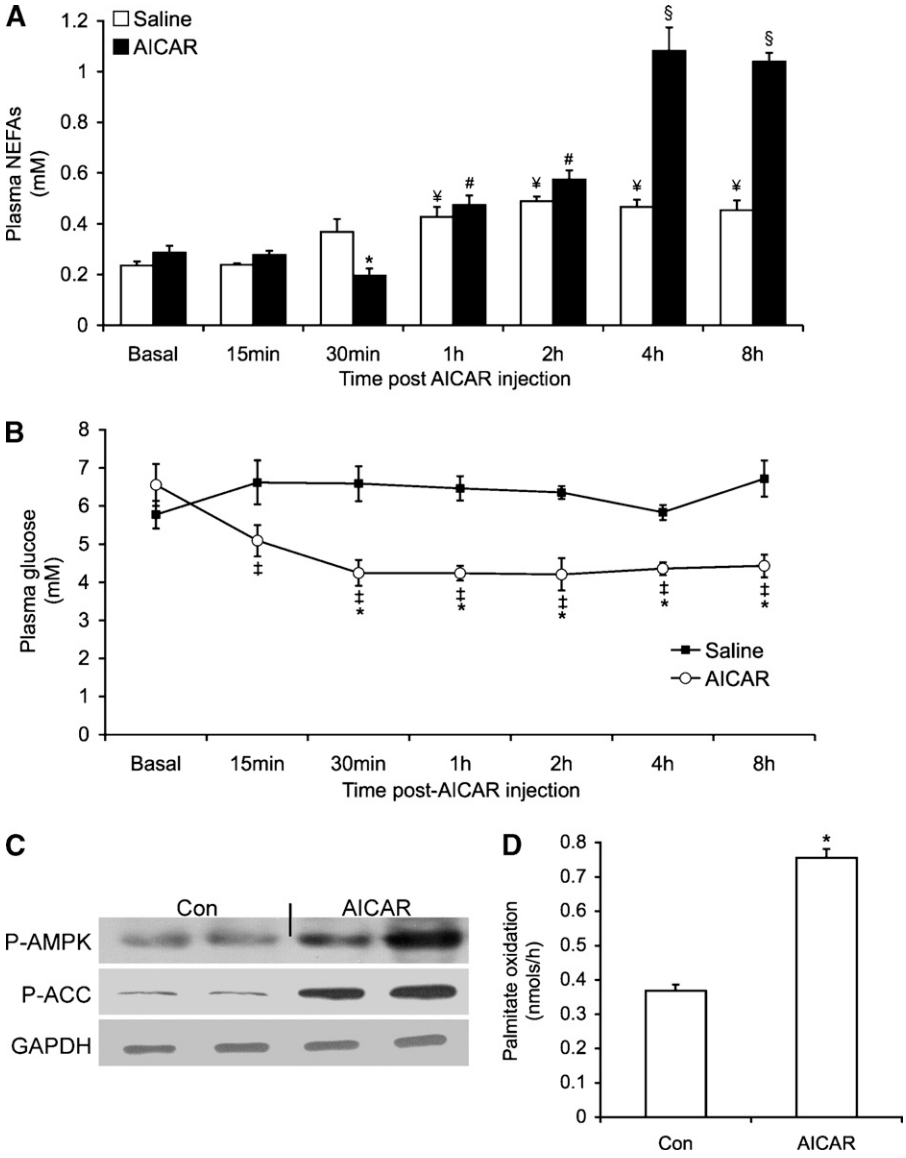

Fig. 5. Time course of NEFAs (A) and plasma glucose levels (B) after AICAR injection. (C) Phosphorylation and content of AMPK. (D) $^{14}CO_2$ production from [1-^{14}C]palmitic acid from epididymal fat pads of AICAR-injected rats (0.7 g/kg body weight). Control (Con) rats (white bars) were injected with saline solution. For NEFA determination, blood samples were taken at various time points after injection with saline or AICAR. For P-AMPK and P-ACC, adipocytes were isolated from epididymal fat pads and prepared for Western blotting analyses. Blots are representative of three independent experiments. All other data were compiled from three to four independent experiments, with n = 12–15 for each condition. Unpaired *t*-tests and one-way ANOVAs were performed for statistical analyses. Data for NEFAs, glucose, and palmitate oxidation were compiled from three to four independent experiments, with n = 5–8 for each condition. Error bars represent SEM. $^{*}P < 0.05$ versus Con and basal values. $^{\#}P < 0.05$ versus 0, 15, and 30 min. $^{¥}P < 0.05$ versus Con. $^{§}P < 0.05$ versus 0, 15 min, 30 min, 1 h, and 2 h. $^{‡}P < 0.05$ versus relative saline control.

treatment significantly inhibited phosphorylation of HSL_{563} and HSL_{660} under basal and epinephrine-stimulated conditions (Fig. 4A), whereas it increased phosphorylation of the HSL_{565} residue (Fig. 4A). In cells exposed to AICAR, basal HSL activity significantly decreased by ~40%, whereas the epinephrine-stimulated effect was suppressed by ~60% (Fig. 4B), despite the fact that total HSL content increased by ~2-fold (Fig. 4A). Furthermore, ATGL, which is a TAG-specific lipase, showed a time-dependent increase in its content (Fig. 4D), reaching ~4-fold greater than control values in AICAR-treated cells (Fig. 4C). TAG lipase activity was increased from 9.1 ± 0.8 pmol/min to 12.8 ± 0.3 pmol/min in control versus AICAR-treated cells, respectively (Fig. 4E).

Time course of plasma glucose and NEFAs, measurement of AMPK/ACC phosphorylation, and determination of palmitate oxidation in WAT after AICAR injection

Basal plasma NEFA concentrations decreased by ~55% 30 min after AICAR injection (**Fig. 5A**). However, NEFA release increased in a time-dependent manner, reaching values ~2.4- and ~2.1-fold higher than control at 4 h and 8 h, respectively (Fig. 5A). Plasma glucose was significantly reduced, from 6.6 to 4.2, 4.2, 4.2, 4.3, and 4.4 mM at 30 min, 1 h, 2 h, 4 h, and 8 h after AICAR injection, respectively (Fig. 5B). No alteration in plasma glucose was observed in saline-injected animals throughout the same time period (Fig. 5B). AMPK phosphorylation increased by ~14-fold in epididymal fat tissue of AICAR-injected animals, whereas total content of this protein was unchanged (Fig. 5C). Palmitate oxidation was increased by ~2.2-fold in adipocytes isolated from epididymal fat pads of AICAR-treated rats (Fig. 5D). These results indicate that exposure of isolated adipocytes to AICAR for 15 h caused similar effects in lipolysis, AMPK activation, and FA oxidation as observed in adipocytes isolated from rats 15 h after AICAR injection.

DISCUSSION

Here, we demonstrate the novel finding that chronic AMPK activation remodels adipocyte metabolism by preventing TAG storage and by activating pathways that promote energy dissipation within the adipocyte. This is supported by a powerful suppression (~60%) in FA uptake and by an ~3.5- and 6-fold increase in exogenous and endogenous FA oxidation induced by AICAR, respectively. The expression of AMPKα2, PGC-1α, PPARα, and PPARδ, which are directly implicated in the expression of enzymes of FA oxidation and mitochondrial biogenesis (6, 7, 23), were upregulated after 15 h of AICAR treatment. Additionally, mRNA of cytochrome C oxidase, CPT-1b, and acetyl-CoA oxidase was upregulated with AICAR treatment. Compatible with these findings was an elevation (~1.9-fold) in citrate synthase activity after 15 h of AICAR treatment, indicating that metabolism was being diverted toward β-oxidation of FAs. Furthermore, the content of the lipogenic enzyme ACC was significantly reduced, whereas its phosphorylation state was increased. This is compatible with an increase in FA oxidation from in vitro and in vivo AICAR-treated adipocytes. We found that chronic AICAR-induced AMPK activation increased (~4.8-fold) the expression of the AMPKα2 subunit without affecting mRNA levels of the α1 isoform. This was accompanied by a significant time-dependent increase in AMPK and PGC-1α content, which is in line with the increase in FA oxidation observed in this study. The mRNA content of the lipogenic transcription factor PPARγ was significantly increased by AICAR treatment. However, our functional data clearly indicate that lipid synthesis and storage are strongly inhibited in adipocytes exposed to AICAR. This could be explained by the fact that induction of PGC-1α by AMPK activation, combined with an increase in PPARα and PPARδ expression, overrides the potential lipogenic effects of PPARγ in AICAR-treated white adipocytes.

A surprising finding of our study was that acute and chronic AICAR-induced AMPK activation suppressed glycerol release under basal and epinephrine-stimulated conditions. However, when we assessed lipolysis by measuring NEFAs in the medium, we found that it was initially reduced after AICAR treatment but progressively increased in a time-dependent manner, reaching values ~10- and ~1.8-fold higher than controls at 15 h under basal and epinephrine-stimulated conditions, respectively. These findings were also reproduced in vivo when we determined the time course of NEFAs in the plasma of AICAR-injected rats over an 8 h time period. The reduction in glycerol release

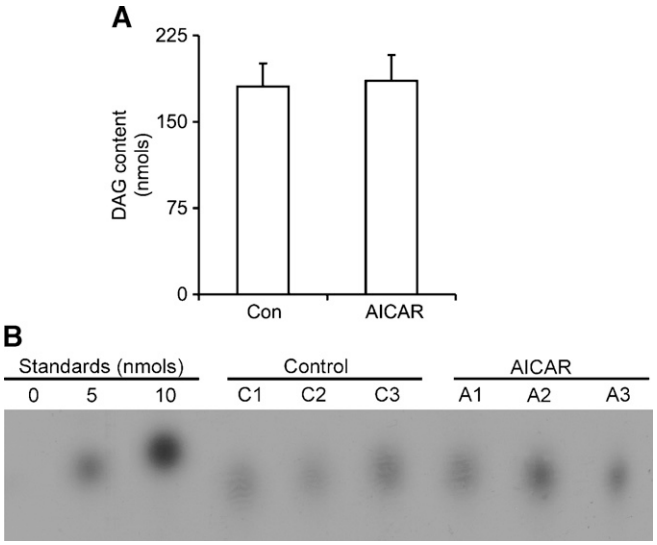

Fig. 6. Quantification of cellular diacylglycerol (DAG) levels (A) and representative TLC plate visualized by autoradiography (B). Isolated adipocytes were incubated in the absence or presence of AICAR (0.5 mM) for 15 h, and lipids were extracted and subjected to the DAG kinase assay for conversion of DAG into phosphatidic acid. Lipids were separated by TLC, and spots corresponding to phosphatidic acid were scraped off and counted for radioactivity. DAG standards of 0, 5, and 10 nmol were assayed concurrently with samples for absolute quantification. C1–C3 and A1–A3 refer to control and AICAR samples, respectively. Data for DAG quantification are representative of three independent experiments, with n = 9 for each condition. Unpaired *t*-test was used for statistical analysis. Error bars represent SEM.

by adipocytes could have been because reesterification of FAs was upregulated in cells chronically exposed to AICAR. To test this hypothesis, GyK activity, PEPCK-1 expression, and the incorporation of palmitate, glucose, pyruvate, and glycerol into lipids were determined. We found that the activity of GyK was not affected in isolated adipocytes treated with AICAR, whereas the incorporation of glycerol into lipids was reduced by ~35%. Also, in line with these findings was the observation that glucose incorporation into lipids was powerfully suppressed with AICAR treatment, indicating a decrease in lipogenesis. Alternatively, reesterification of FAs could also occur through glyceroneogenesis, leading to FA recycling in adipocytes (24). We found that mRNA levels of PEPCK-1, the cytosolic form of PEPCK, were increased by 7-fold, and protein levels were clearly enhanced with chronic AICAR treatment, suggesting upregulation of glyceroneogenesis. However, the incorporation of palmitate into lipids indicated that even though the glyceroneogenic pathway could be upregulated, reesterification of FA was decreased by ~70% with AICAR treatment. This correlates with in vivo studies from our lab (unpublished observations) and others (20) demonstrating that chronic AICAR injections in rats cause a decrease in fat mass (subcutaneous, epididymal, and retroperitoneal depots), further supporting a decrease in TG storage. Furthermore, our in vitro and in vivo measurements of NEFAs were still substantially increased after 15 h of AICAR treatment, indicating a lack of FA recycling back into TAG in the adipose tissue. Therefore, FA reesterification could not account for the lower glycerol release observed after AICAR treatment. In this scenario, incomplete lipolysis could be occurring, which could explain the increase in NEFAs without a concomitant increase in glycerol release. To test this, we examined phosphorylation and activity of HSL. We found that chronic treatment of white adipocytes with AICAR significantly increased HSL phosphorylation at Ser565, whereas phosphorylation of the PKA-dependent Ser563 and Ser660 was powerfully suppressed, despite the fact that total HSL content was increased. Furthermore, this was accompanied by a significant reduction of ~40% in basal HSL activity and ~60% inhibition of epinephrine-induced HSL activation. Even though HSL plays an important role in lipolysis, a new TAG-specific lipase, ATGL, has recently been identified. Ablation of ATGL significantly decreased the release of glycerol and FAs from fat cells (25, 26); therefore, it has been proposed that complete hydrolysis of TAG in adipocytes requires the expression and activation of both acyl hydrolases (27). Here, we provide evidence that AICAR-induced AMPK activation suppressed the activity of HSL, but promoted an ~4-fold increase in ATGL content in adipocytes. Although we were unable to obtain a direct measurement of ATGL activity, the increase in total TAG lipase

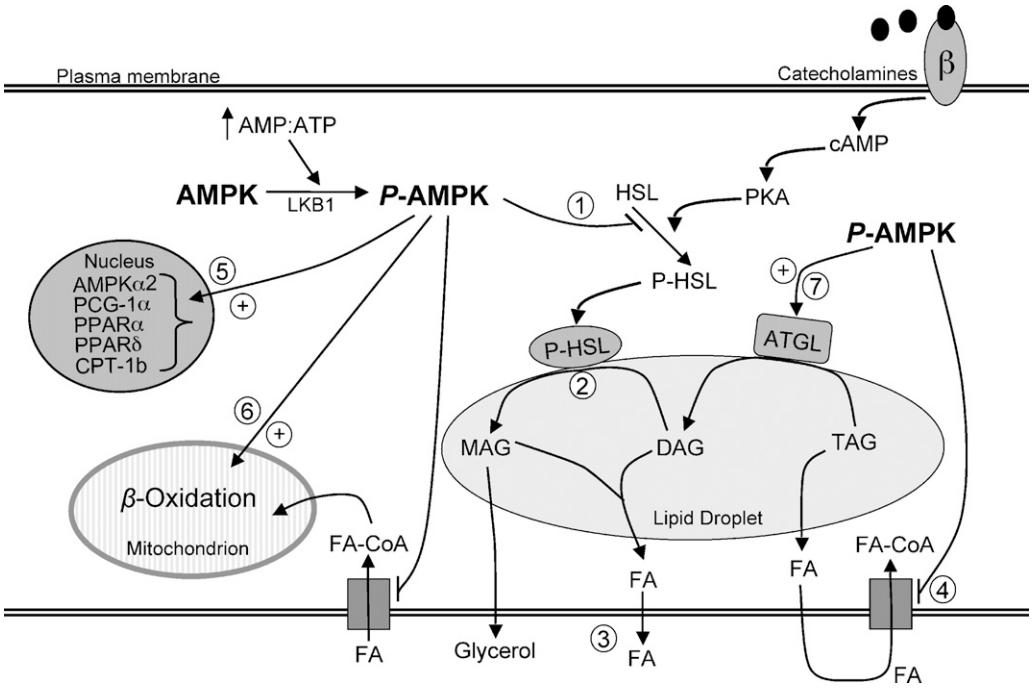

Fig. 7. The role of AMPK activation in lipid metabolism in white adipocytes. Acute activation of AMPK inhibits HSL activity (1), which prevents hydrolysis of DAG (2) and subsequent liberation of glycerol and FAs (3). Acute and chronic pharmacological AMPK activation powerfully suppresses FA uptake (4), conferring an anti-lipogenic role for AMPK in white adipose tissue. Furthermore, chronic AMPK activation upregulates the expression of genes (PGC-1α, PPARα, PPARδ, CPT-1b) (5) that increase the ability of the cell to dispose of FAs intracellularly through β-oxidation (6). ATGL content is also increased with AMPK activation (7) and catalyzes the hydrolysis of one FA from TAG. ⊕ and → denote stimulation; ⟞ denotes inhibition. MAG, monoacylglycerol; LKB1, AMPK kinase.

activity (~40%) indicates that the increase in ATGL content must have facilitated the initiation of TAG hydrolysis but that the inhibition of HSL activation may have restricted further breakdown of DAG. This is in line with the time-dependent elevation of FA release without a concomitant increase in glycerol levels observed in the present study. Measurement of DAG levels in the cell showed no differences between control and AICAR-treated cells (**Fig. 6**). It could be that the accumulation of DAG in AICAR-treated cells is not sufficient to detect a difference after only 15 h of treatment. In fact, studies using HSL knock-out mice indicate that only after 16 weeks is DAG accumulation detected in WAT of these mice (28). It is also possible that any excess DAG being produced may be diverted toward pathways where DAG molecules can be quickly converted into ceramides or various phospholipid molecules (29). Importantly, the assay used by us to quantify cellular DAG content is also suitable for measuring ceramide production, and we were not able to detect a significant amount of it in either control or AICAR-treated cells (Fig. 6). Therefore, the ultimate fate of DAG, if it indeed accumulates and/or is shunted toward an alternative pathway, requires further investigation.

It is important to highlight that the effect of AICAR on FA release was time dependent. Shortly after initiation of AICAR treatment, lipolysis was decreased, as shown by NEFA release both in vitro and in vivo, which can be attributed to the rapid inhibition by AMPK of HSL phosphorylation/activity. However, because changes in gene expression and protein content take longer to occur, the effects of increased ATGL content on lipolysis were evident only 4–6 h after AICAR treatment. Previous studies have assessed the effect of AMPK activation on lipolysis in adipocytes in vitro (27, 30–32) by measuring glycerol release and have reported conflicting results regarding whether AMPK is pro- or antilipolytic. Our data provide a novel mechanism by which AMPK exerts time-dependent effects on lipolysis, which could only be detected by measuring the release of both glycerol and NEFAs. Therefore, future studies investigating the role of prolonged AMPK activation in lipolysis should not rely on glycerol release as the sole indicator of TAG breakdown.

The elevated levels of NEFAs in AICAR-injected animals raise the possibility that chronic pharmacological activation of AMPK in WAT may lead to lipotoxicity and contribute to the development of insulin resistance. However, our data indicate that plasma glucose levels in fed animals significantly decreased (~35%) after AICAR injection, suggesting that glucose uptake in peripheral tissues was increased. Furthermore, the effect of AICAR on plasma glucose clearance was so potent that fasted animals had to be euthanized 1 h after injection of this AMPK agonist due to severe hypoglycemia (data not shown). Also in line with these findings, several long-term in vivo studies using lean and diabetic rodent models have shown that AICAR-induced AMPK activation significantly reduces plasma glucose levels (19, 33, 34), indicating that despite elevated NEFA levels, glucose homeostasis is improved with treatment using this AMPK agonist. Additionally, activation of AMPK increases FA oxidation in peripheral tissues such as liver and skeletal muscle (1), thereby exerting an anti-lipotoxic effect by preventing the accumulation of lipids in nonadipose tissues.

Even though lipolysis may be seen as a pathway that provides substrate for tissues to produce ATP and maintain cellular energy homeostasis, activation of AMPK has been proposed to limit lipolysis in WAT and actually spare energy (2). The rationale for this is based on the fact that if FAs released by lipolysis are not oxidized either within the adipocyte or in other tissues, they are recycled into TAGs in the fat cells, creating a "futile cycle" (10). Therefore, AMPK activation as a consequence of lipolysis has been proposed to operate as a mechanism to restrain energy depletion in WAT (35). On the basis of our data, we propose that chronic AMPK activation remodels adipocyte metabolism, which may restrict energy depletion and increase ATP production. When acutely activated in the adipocyte, AMPK quickly inhibits HSL activity and also suppress glucose and FA uptake (3). These rapid effects may be important to limiting the excessive release of FAs and the potential energy cost of reesterifying FAs that are not disposed of internally or peripherally (**Fig. 7**). If chronically activated, AMPK also promotes alterations in gene expression that increase the ability of the cell to dispose of FAs internally through oxidation, facilitating ATP production and maintenance of intracellular energy homeostasis (Fig. 7). In our experiments, these chronic adaptations led to a net time-dependent increase in vitro and in vivo of FA release, indicating that the WAT can cope with internal energy challenges without compromising the provision of substrate for energy production in peripheral tissues. In summary, novel evidence is provided that through chronic pharmacological activation of AMPK, WAT metabolism may be remodeled toward energy dissipation rather than storage. AMPK exerts these effects through distinct time-dependent regulation of HSL and ATGL, and by altering the expression of genes that promote lipid utilization versus storage in adipocytes. These mechanisms may be of great relevance for the treatment of obesity and type 2 diabetes.

REFERENCES

1. Long, Y. C., and J. R. Zierath. 2006. AMP-activated protein kinase signaling in metabolic regulation. *J. Clin. Invest.* **116:** 1776–1783.
2. Hardie, D. G. 2007. AMP-activated protein kinase as a drug target. *Annu. Rev. Pharmacol. Toxicol.* **47:** 185–210.
3. Gaidhu, M. P., S. Fediuc, and R. B. Ceddia. 2006. 5-Aminoimidazole-4-carboxamide-1-beta-D-ribofuranoside-induced AMP-activated protein kinase phosphorylation inhibits basal and insulin-stimulated glucose uptake, lipid synthesis, and fatty acid oxidation in isolated rat adipocytes. *J. Biol. Chem.* **281:** 25956–25964.
4. Fediuc, S., A. S. Pimenta, M. P. Gaidhu, and R. B. Ceddia. 2008. Activation of AMP-activated protein kinase, inhibition of pyruvate dehydrogenase activity, and redistribution of substrate partitioning mediate the acute insulin-sensitizing effects of troglitazone in skeletal muscle cells. *J. Cell. Physiol.* **215:** 392–400.
5. Salt, I., J. W. Celler, S. A. Hawley, A. Prescott, A. Woods, D. Carling, and D. G. Hardie. 1998. AMP-activated protein kinase: greater AMP dependence, and preferential nuclear localization, of complexes containing the alpha2 isoform. *Biochem. J.* **334:** 177–187.
6. Orci, L., W. S. Cook, M. Ravazzola, M. Y. Wang, B. H. Park, R. Montesano, and R. H. Unger. 2004. Rapid transformation of white

adipocytes into fat-oxidizing machines. *Proc. Natl. Acad. Sci. USA.* **101:** 2058–2063.
7. Wang, M. Y., L. Orci, M. Ravazzola, and R. H. Unger. 2005. Fat storage in adipocytes requires inactivation of leptin's paracrine activity: implications for treatment of human obesity. *Proc. Natl. Acad. Sci. USA.* **102:** 18011–18016.
8. Chen, G., K. Koyama, X. Yuan, Y. Lee, Y. T. Zhou, R. O'Doherty, C. B. Newgard, and R. H. Unger. 1996. Disappearance of body fat in normal rats induced by adenovirus-mediated leptin gene therapy. *Proc. Natl. Acad. Sci. USA.* **93:** 14795–14799.
9. Canová, N., D. Lincová, and H. Farghali. 2005. Inconsistent role of nitric oxide on lipolysis in isolated rat adipocytes. *Physiol. Res.* **54:** 387–393.
10. Guan, H. P., Y. Li, M. V. Jensen, C. B. Newgard, C. M. Steppan, and M. A. Lazar. 2002. A futile metabolic cycle activated in adipocytes by antidiabetic agents. *Nat. Med.* **8:** 1122–1128.
11. Dole, V. P., and H. Meinertz. 1960. Microdetermination of long-chain fatty acids in plasma and tissues. *J. Biol. Chem.* **235:** 2595–2599.
12. William, W. N. J., R. B. Ceddia, and R. Curi. 2002. Leptin controls the fate of fatty acids in isolated rat white adipocytes. *J. Endocrinol.* **175:** 735–744.
13. Bligh, E. G., and W. J. Dyer. 1959. A rapid method of total lipid extraction and purification. *Can. J. Biochem. Physiol.* **37:** 911–917.
14. Wang, T., Y. Zang, W. Ling, B. E. Corkey, and W. Guo. 2003. Metabolic partitioning of endogenous fatty acid in adipocytes. *Obes. Res.* **11:** 880–887.
15. Alp, P. R., E. A. Newsholme, and V. A. Zammit. 1976. Activities of citrate synthase and NAD+-linked and NADP+-linked isocitrate dehydrogenase in muscle from vertebrates and invertebrates. *Biochem. J.* **154:** 689–700.
16. Preiss, J., C. R. Loomis, W. R. Bishop, R. Stein, J. E. Niedel, and R. M. Bell. 1986. Quantitative measurement of sn-1,2-diacylglycerols present in platelets, hepatocytes, and ras- and sis-transformed normal rat kidney cells. *J. Biol. Chem.* **261:** 8597–8600.
17. Fediuc, S., M. P. Gaidhu, and R. B. Ceddia. 2006. Inhibition of insulin-stimulated glycogen synthesis by 5-aminoimidasole-4-carboxamide-1-beta-d-ribofuranoside-induced adenosine 5′-monophosphate-activated protein kinase activation: interactions with Akt, glycogen synthase kinase 3-3alpha/beta, and glycogen synthase in isolated rat soleus muscle. *Endocrinology.* **147:** 5170–5177.
18. Pold, R., L. S. Jensen, N. Jessen, E. S. Buhl, O. Schmitz, A. Flyvbjerg, N. Fujii, L. J. Goodyear, C. F. Gotfredsen, C. L. Brand, et al. 2005. Long-term AICAR administration and exercise prevents diabetes in ZDF rats. *Diabetes.* **54:** 928–934.
19. Song, X. M., M. Fiedler, D. Galuska, J. W. Ryder, M. Fernstrom, A. V. Chibalin, H. Wallberg-Henriksson, and J. R. Zierath. 2002. 5-Aminoimidazole-4-carboxamide ribonucleoside treatment improves glucose homeostasis in insulin-resistant diabetic (ob/ob) mice. *Diabetologia.* **45:** 56–65.
20. Winder, W. W., B. F. Holmes, D. S. Rubink, E. B. Jensen, M. Chen, and J. O. Holloszy. 2000. Activation of AMP-activated protein kinase increases mitochondrial enzymes in skeletal muscle. *J. Appl. Physiol.* **88:** 2219–2226.
21. Danguir, J., and S. Nicolaidis. 1980. Circadian sleep and feeding patterns in the rat: possible dependence on lipogenesis and lipolysis. *Am. J. Physiol.* **238:** E223–E230.
22. Fredrikson, G., P. Stralfors, N. O. Nilsson, and P. Belfrage. 1981. Hormone-sensitive lipase from adipose tissue of rat. *Methods Enzymol.* **71:** 636–646.
23. Jager, S., C. Handschin, J. St-Pierre, and B. M. Spiegelman. 2007. AMP-activated protein kinase (AMPK) action in skeletal muscle via direct phosphorylation of PGC-1alpha. *Proc. Natl. Acad. Sci. USA.* **104:** 12017–12022.
24. Reshef, L., Y. Olswang, H. Cassuto, B. Blum, C. M. Croniger, S. C. Kalhan, S. M. Tilghman, and R. W. Hanson. 2003. Glyceroneogenesis and the triglyceride/fatty acid cycle. *J. Biol. Chem.* **278:** 30413–30416.
25. Schweiger, M., R. Schreiber, G. Haemmerle, A. Lass, C. Fledelius, P. Jacobsen, H. Tornqvist, R. Zechner, and R. Zimmermann. 2006. Adipose triglyceride lipase and hormone-sensitive lipase are the major enzymes in adipose tissue triacylglycerol catabolism. *J. Biol. Chem.* **281:** 40236–40241.
26. Zimmermann, R., G. Haemmerle, E. M. Wagner, J. G. Strauss, D. Kratky, and R. Zechner. 2003. Decreased fatty acid esterification compensates for the reduced lipolytic activity in hormone-sensitive lipase-deficient white adipose tissue. *J. Lipid Res.* **44:** 2089–2099.
27. Duncan, R. E., M. Ahmadian, K. Jaworski, E. Sarkadi-Nagy, and H. S. Sul. 2007. Regulation of lipolysis in adipocytes. *Annu. Rev. Nutr.* **27:** 79–101.
28. Haemmerle, G., R. Zimmermann, M. Hayn, C. Theussl, G. Waeg, E. Wagner, W. Sattler, T. M. Magin, E. F. Wagner, and R. Zechner. 2002. Hormone-sensitive lipase deficiency in mice causes diglyceride accumulation in adipose tissue, muscle, and testis. *J. Biol. Chem.* **277:** 4806–4815.
29. Carrasco, S., and I. Merida. 2007. Diacylglycerol, when simplicity becomes complex. *Trends Biochem. Sci.* **32:** 27–36.
30. Daval, M., F. Foufelle, and P. Ferre. 2006. Functions of AMP-activated protein kinase in adipose tissue. *J. Physiol.* **574:** 55–62.
31. Sullivan, J. E., K. J. Brocklehurst, A. E. Marley, F. Carey, D. Carling, and R. K. Beri. 1994. Inhibition of lipolysis and lipogenesis in isolated rat adipocytes with AICAR, a cell-permeable activator of AMP-activated protein kinase. *FEBS Lett.* **353:** 33–36.
32. Yin, W., J. Mu, and M. J. Birnbaum. 2003. Role of AMP-activated protein kinase in cyclic AMP-dependent lipolysis In 3T3-L1 adipocytes. *J. Biol. Chem.* **278:** 43074–43080.
33. Bergeron, R., S. F. Previs, G. W. Cline, P. Perret, R. R. Russell III, L. H. Young, and G. I. Shulman. 2001. Effect of 5-aminoimidazole-4-carboxamide-1-beta-D-ribofuranoside infusion on in vivo glucose and lipid metabolism in lean and obese Zucker rats. *Diabetes.* **50:** 1076–1082.
34. Koistinen, H. A., D. Galuska, A. V. Chibalin, J. Yang, J. R. Zierath, G. D. Holman, and H. Wallberg-Henriksson. 2003. 5-Amino-imidazole carboxamide riboside increases glucose transport and cell-surface GLUT4 content in skeletal muscle from subjects with type 2 diabetes. *Diabetes.* **52:** 1066–1072.
35. Gauthier, M. S., H. Miyoshi, S. C. Souza, J. M. Cacicedo, A. K. Saha, A. S. Greenberg, and N. B. Ruderman. 2008. AMP-activated protein kinase is activated as a consequence of lipolysis in the adipocyte: potential mechanism and physiological relevance. *J. Biol. Chem.* **283:** 16514–16524.